01 Aug 2007

Hand-Assembled Cable Bundle Modeling for Crosstalk and Common-Mode Radiation Prediction

Shishuang Sun

Geping Liu

James L. Drewniak
Missouri University of Science and Technology, drewniak@mst.edu

David Pommerenke
Missouri University of Science and Technology, davidjp@mst.edu

Recommended Citation

S. Sun et al., "Hand-Assembled Cable Bundle Modeling for Crosstalk and Common-Mode Radiation Prediction," *IEEE Transactions on Electromagnetic Compatibility*, vol. 49, no. 3, pp. 708-718, Institute of Electrical and Electronics Engineers (IEEE), Aug 2007.
The definitive version is available at https://doi.org/10.1109/TEMC.2007.897142

Hand-Assembled Cable Bundle Modeling for Crosstalk and Common-Mode Radiation Prediction

Shishuang Sun, *Member, IEEE*, Geping Liu, James L. Drewniak, *Senior Member, IEEE*, and David J. Pommerenke, *Senior Member, IEEE*

***Abstract*—A statistical cable bundle model is developed to account for the random disturbance of the wire positions along hand-assembled cable bundles. The nonuniform random bundles are modeled as n-cascaded segments of a uniform multiconductor transmission line. At each section, all wire positions are disturbed with random numbers obeying a Gaussian distribution. In addition, a spline interpolation function is used to improve the continuity of wires winding along the bundle. The wire crosstalk and the common-mode (CM) current distribution along the bundle can be calculated with simulation program with integrated circuit emphasis (SPICE)-like solvers. By injecting the CM current along the bundle into a full-wave tool, e.g., finite-difference time domain (FDTD), as impressed current sources, the system-level electromagnetic emissions from the cable bundles can be predicted. The model has been experimentally validated with a controlled laboratory setup.**

***Index Terms*—Cable bundles, common-mode (CM) current, crosstalk, electromagnetic interference (EMI), multiconductor transmission line (MTL), statistical.**

I. Introduction

HAND-ASSEMBLED cable bundles are one of the primary means of interconnections among modern electronic devices in transport and industrial applications. With increasing clock frequency and more dense electronic devices, the modeling of electromagnetic emissions from cable bundles becomes more important because the electromagnetic interference (EMI) poses great challenges for the compliance of commercial products with EMI limits, and crosstalk and EMI also cause electronic equipment malfunctions that may be a safety issue. For modeling a typical hand-assembled cable bundle, one of the challenges is that hand-assembled cable bundles show great variability on the positions of the wires within cable bundles because of the random nature of the bundle assembly. This lack of uniformity precludes any rigorous deterministic analysis. Therefore, a statistical approach must be employed to account for the intrinsic random behavior of cable bundles. The essence of modeling a random cable bundle is to generate a set of nonuniform cable bundles whose realizations are different from each other. For each specific realized bundle, which is deterministic but nonuniform, it can be solved with either analytical solutions of nonuniform bundles developed based on a multiconductor transmission line (MTL) theory [1]–[3], or an MTL model of simulation program with integrated circuit emphasis (SPICE) solvers by approximating the bundle with cascaded uniform segments. A SPICE-solver is employed herein to perform the simulations.

Two cable harness modeling methods have previously been reported in the literatures to statistically represent the random behavior of hand-assembled cable bundles. In [4], a Monte Carlo algorithm was introduced. The cable bundle is divided into n uniform segments whose 2-D cross sections are identical, but the positions of the wires are randomly interchanged from segment to segment. The continuity of the wire routing can only be loosely controlled with the total number of segments. The random midpoint displacement (RMD) algorithm is another method [5]–[7] that also divides the bundle into n uniform cascaded segments, but describes the positions of a wire along a bundle with a fractal curve. The continuity of the wires within cable bundles is controlled through the fractal dimension and the total number of segments. The RMD method gives a better representation of an actual cable bundle in terms of continuity, and it has more flexibility to control the randomness of the wires. However, because of the nature of the algorithms, the constructed wires with both methods result in unphysical large discontinuities between adjacent bundle segments. The large discontinuities result in unphysical resonances of the common-mode (CM) current along cable bundles, which compromises the effectiveness of both models, especially at high frequency. To mitigate the discontinuities and more physically represent an actual cable bundle behavior, a new method, i.e., the random displacement spline interpolation (RDSI) algorithm, is proposed and developed in this paper. In Section II, the RDSI algorithm is briefly introduced. In Section III, the wire crosstalk, the CM current along the bundle, and the resulting electric field are predicted with the RDSI cable harness model. A detailed statistical analysis of the simulation results is performed. In Section IV, a test setup in a controlled laboratory environment is used to assess the effectiveness of the RDSI cable harness model. In Section V, the engineering implications of modeling random cable bundles are discussed. Finally, the performance of the RDSI cable bundle model is summarized in Section VI.

II. RDSI Algorithm Description

The bundle realization with the RDSI algorithm is described with a single-wire construction. Assume the bundle is along

Manuscript received June 23, 2006.

S. Sun and G. Liu are with the Characterization Group, Altera Corporation, San Jose, CA 95134 USA (e-mail: ssun@altera.com; gliu@altera.com).

J. L. Drewniak and D. J. Pommerenke are with the Electrical Engineering Department, University of Missouri-Rolla, Rolla, MO 65409 USA (e-mail: drewniak@ umr.edu; davidjp@umr.edu).

Digital Object Identifier 10.1109/TEMC.2007.897142

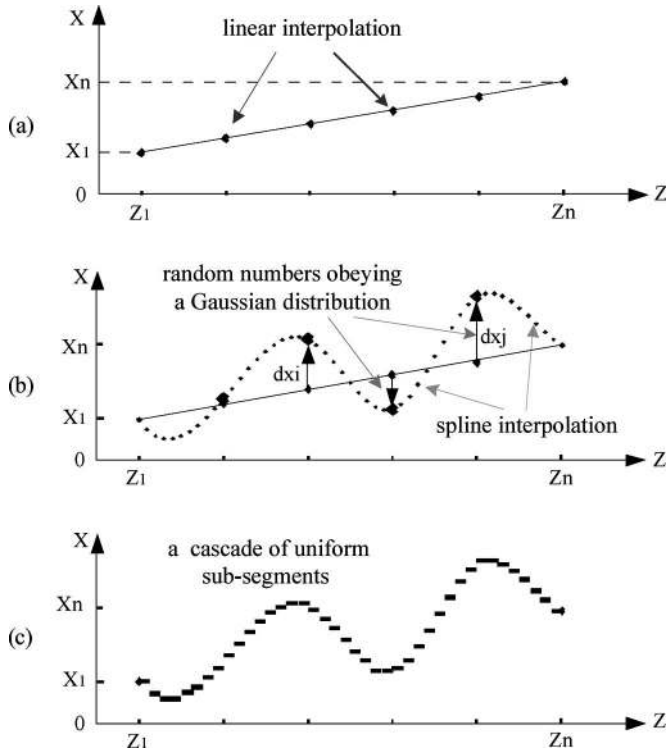

Fig. 1. Schematic illustration of wire modeling using the RDSI algorithm.

the z-axis, and the wire is divided into n uniform segments. The wire position along the bundle can be represented as a set of (x_i, y_i, z_i) coordinates, where i is the 2-D cross section number. The reference point could be anywhere, but it was chosen as the center point of the start end of the bundle herein just for simplicity. The x_i- and y_i-coordinates determine the 2-D cross-sectional position of the wire at the ith segment. The length of each segment is $1/n$ times the length of the bundle. Fig. 1 shows the mechanism of the wire modeling within the bundle using the RDSI algorithm. For simplicity, only the x-coordinate generation along the z-axis is shown in the figure. The y-coordinate generation follows in an identical fashion.

There are four steps to construct the wire representation within a bundle. To simplify the method at this stage, two assumptions are made in the implementation of the proposed algorithm. First, the diameters of all the wires inside the bundle are the same; so, any two wires are interchangeable. Second, the overall geometry of the 2-D cross section of the bundle is invariant along the axial direction, and the positions of the realized wires are allowed only within the predefined wire locations. Therefore, the evaluation of the per-unit-length (p.u.l) L & C matrices needs only to be performed once because of the invariant 2-D cross section. This restriction is not essential, but lifting it significantly increases the computation time. In practice, this assumption may result in some error. However, when the wires are densely packed, and the number of the wires is up to hundreds, two arbitrary cross sections of a random bundle should be approximately the same. The key point of this model is to determine the mutual spacing between wires. Note that the RDSI algorithm does not preclude the modeling of cable harnesses whose wires have different diameters.

Step 1: Initial Spline Coordinate Calculation

The wire is first divided into n rather long segments, which are referred to as spline segments. The length of each segment is approximately the same as the twist length of the actual cable harnesses under investigation. As shown in Fig. 1(a), the coordinates of the midpoints of the spline segments are calculated using linear interpolation according to the coordinates of the two ends of the wire, which can be measured from the connectors at the two ends of the bundle.

Step 2: Spline Coordinate Randomization

In the second step, random numbers from a Gaussian distribution are generated. The final coordinates of the spline segments are the summation of the initial coordinates and the random numbers. Then, all spline segments along the sequential line are displaced using the Gaussian distribution. The mean of the Gaussian distribution is zero; so, the standard deviation of the random numbers is the key parameter that controls the randomness of the wire positions. This process is shown in Fig. 1(b).

Step 3: Spline Interpolation

In the third step, the wire is further divided into uniform subsegments. There are two criteria to determine the length of subsegments. The first criterion is that the length should be equal to or less than one-tenth of the shortest wavelength of interest, which ensures the spatial resolution of the wave with the highest frequency of interest. The second criterion is that one spline segment should have ten or more subsegments to improve the continuity of the constructed wire within the bundle. Both criteria need to be satisfied, so, the smaller one of the two subsegment lengths will be used. With coordinates of the spline segments available, the coordinates of the subsegments of the wire can be generated using a piecewise polynomial form of a cubic spline interpolation technique, as shown in Fig. 1(c).

Step 4: Fitting the Generated Wires Into the Bundle

The coordinates of the wire at each cross section are generated at this junction. The last step is to fit the realized wire into the predefined locations at each cross section. The predefined wire locations are used as reference. At the beginning, all the reference positions are unoccupied. Starting with the first wire, from the first 2-D cross section to the last 2-D cross section, the distances between the coordinates of a new wire and all the unoccupied reference locations are calculated and compared. The new wire is placed at the position of the nearest, unoccupied reference location. A reference location is taken, and then identified as occupied. The iterations continue until the last wire is placed at the final unoccupied reference location, and then new 2-D cross sections with identical geometry but different wire positions are generated. In this fashion, the wire is represented as a cascade of short, uniform subsegments. Because of the nature

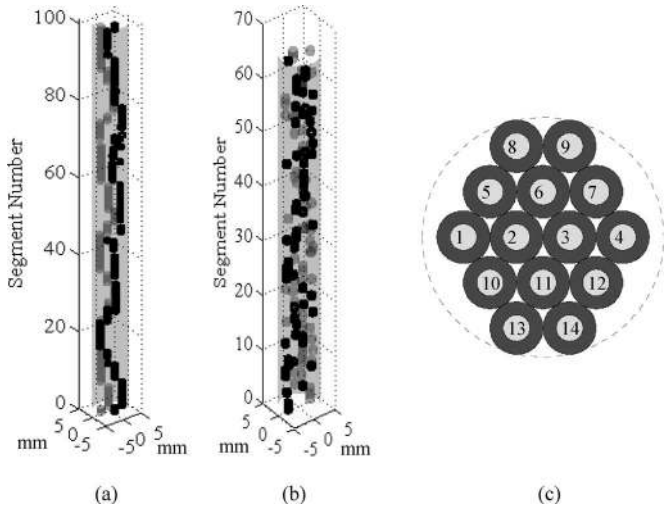

Fig. 2. Three-dimensional visualization of two wires along the bundle that are constructed with the (a) RDSI and (b) RMD algorithms. (c) Two-dimensional cross section. The normalized STDs are all 0.5, and the bundle lengths are both 2 m long.

of the wire representation within the bundle, the new algorithm is further referred to as the RDSI algorithm for simplicity.

The cubic spline interpolation technique improves the continuity of the constructed wire along its length. The constructed wires are more realistic when compared to the actual hand-assembled cable bundle. To visualize the difference of the bundles constructed with the RDSI and RMD algorithms, two arbitrarily chosen wires within a 14-wire bundle are plotted in Fig. 2(a) and (b). Fig. 2(c) shows the 2-D cross-sectional geometry of the bundle. In this figure, the RDSI and RMD algorithms have the same standard deviations (STD) of the wire position displacements. The numbers of segments for the bundles realized with the RMD and RDSI algorithms are 64 and 100, respectively. The large discontinuities between the adjacent subsegments shown in Fig. 2(b) are far from the actual behavior of a cable bundle. This unphysical discontinuity leads to a nonnegligible discrepancy between the actual bundle length geometry and the corresponding resonances of the CM current along the bundle in the simulations. By contrast, the wires constructed with the RDSI algorithm demonstrate a better transition of wire position variation. The RDSI algorithm gives a more physical representation of actual cable bundles.

When the cable bundle is realized, a 2-D quasi-static field solver is used to evaluate the p.u.l. L & C matrices of the 2-D cross-sectional geometry of the bundle used for reference. Since the overall 2-D cross-sectional geometry of the cable bundle is invariant along the cable bundle, and the only difference between any two 2-D cross sections is that the wire positions are interchanged, it is not necessary to calculate the L & C matrices at each 2-D cross section. The matrices can be generated by matrix manipulation according to the relationship between wire positions at the new 2-D cross section and the reference cross section. If the overall 2-D cross-sectional geometry of the cable bundle varies along the bundle, then the p.u.l. L & C matrices need to be evaluated at all the 2-D cross sections that have different cross-sectional geometries. With the knowledge of the L & C matrices of each cross section, and the source and load impedances, SPICE scripts can be generated. The crosstalk between any two wires at any location of the bundle, and the current of each wire at every segment are calculated with a SPICE solver. The CM current is simply the summation of the current of each wire. Herein, a TEM or quasi-TEM mode is implicitly assumed. In a typical case of bundles on an automotive platform, this assumption can be globally satisfied. Repeating the whole process many times, a statistical population of cable bundles and results are generated, and a statistical analysis of the simulation results can be performed.

Height variation of cable bundles resulting from the hand-routing nature can also be easily incorporated in the proposed RDSI algorithm. Following the similar idea of the wire position randomization during the bundle construction, the height of the bundle can be displaced with random numbers obeying a Gaussian distribution, student's T-distribution, etc. The p.u.l. L & C matrices at every 2-D cross section need to be evaluated with a 2-D field solver. However, if a portion of the cable bundle containing many segments has an invariant 2-D cross-sectional geometry before the height of the bundle is randomized, a simplification can be employed to minimize the number of L & C matrices calculations. Suppose the maximum and minimum heights of the bundle can be determined, five or more sets of p.u.l. L & C matrices of this portion of the bundle can be evaluated when the bundle is at the height of its maximum and minimum locations with the other three locations equally spaced in between the maximum and minimum locations. The L & C matrices of the bundle with randomized heights can be linearly interpolated from the five precalculated L & C matrices, or one can simply use the L & C matrices whose corresponding heights are closest to the new randomized heights for further simplification.

III. Numerical Results

The RDSI algorithm described in Section II was applied to a 2-m-long bundle that is composed of 14 AWG #20 wires with polyvinyl chloride (PVC) insulation. The bundle was placed on a rectangular aluminum plate that is 262 cm $\times$ 120 cm. The nominal diameter of the bundle is 8.2 mm, and the average height of the bundle is approximately 2 cm above the aluminum plate. The detailed geometry of the actual measurement setup, and the 2-D cross section of the wire bundle are shown in Fig. 3(a) and (b), respectively. The model parameters are as follows: the standard deviation of the wire position is 0.5; the length of spline segments is 20 cm; and the subsegment length is 2 cm. The CM current was simulated and measured at points P1, P2, and P3. Points P1 and P2 are two arbitrarily chosen points that can represent the general behavior of the bundle. Point P3 was intentionally chosen to be symmetric with respect to the point P1 to investigate the symmetry of the CM current. The electric field was simulated and measured at points P4, P5, and P6.

The bundle was terminated with surface-mount technology (SMT) resistors inside the source and load boxes. The values of

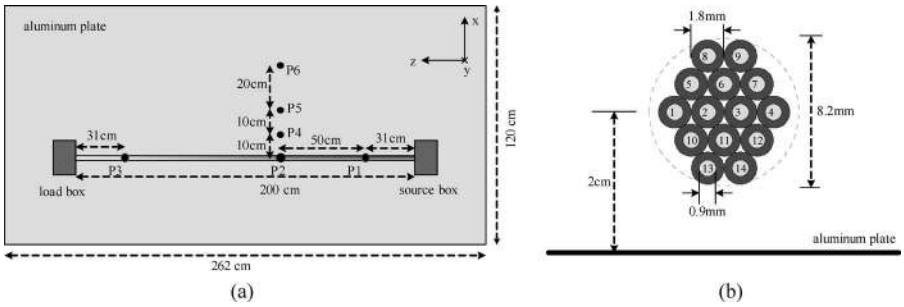

Fig. 3. Schematic of the measurement setup. (a) Top view of the geometry. (b) Two-dimensional cross-sectional view. CM current was simulated and measured at points P1, P2, and P3, and the electric field was simulated and measured at points P4, P5, and P6.

TABLE I
TERMINATIONS OF THE BUNDLE

	Source end	Load end	Relative impedance* Source - Load
Wire1-to-GND	996 Ω	10 Ω	High - Low
Wire 2-to-GND	Feeding (50 Ω)	68 Ω	Low - Low
Wire 3-to-GND	50 Ω	68 Ω	Low - Low
Wire4-to-GND	56 Ω	996 Ω	Low - High
Wire5-to-GND	10 Ω	47 Ω	Low - Low
Wire6-to-GND	1 KΩ	15 KΩ	High – High
Wire7-to-GND	56 Ω	1 KΩ	Low - High
Wire8-to-GND	10 Ω	10 Ω	Low - Low
Wire9-to-GND	15 KΩ	47 Ω	High - Low
Wire10-to-GND	47 Ω	10 Ω	Low - Low
Wire11-to-GND	47 Ω	1 KΩ	Low - High
Wire12-to-GND	10 Ω	100 KΩ	Low – High
Wire13-to-GND	996 Ω	10 Ω	High - Low
Wire14-to-GND	56 Ω	10 Ω	Low - Low

* relative to 100 Ω

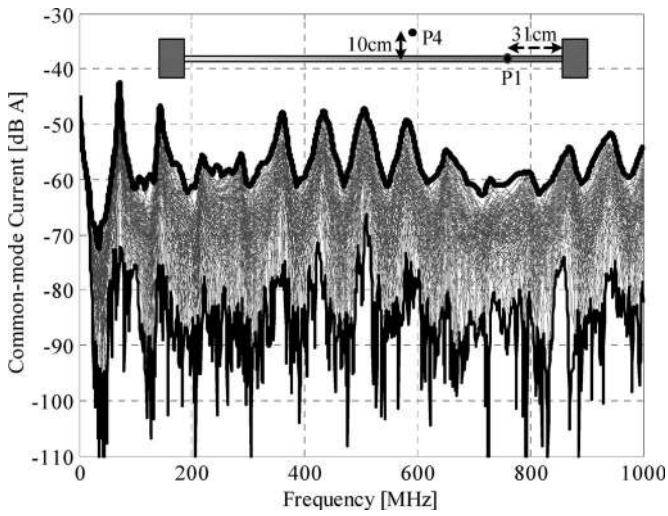

Fig. 4. Simulated CM currents at points P1 with 128 different bundle realizations.

the resistors were randomly chosen as low- and high-impedance combinations with reference to 100 Ω, and they are summarized in Table I. For the feeding wire (wire 2), both the source impedance (50 Ω) and the load impedance (68 Ω) are relatively low impedances; this setup is current-driven in nature.

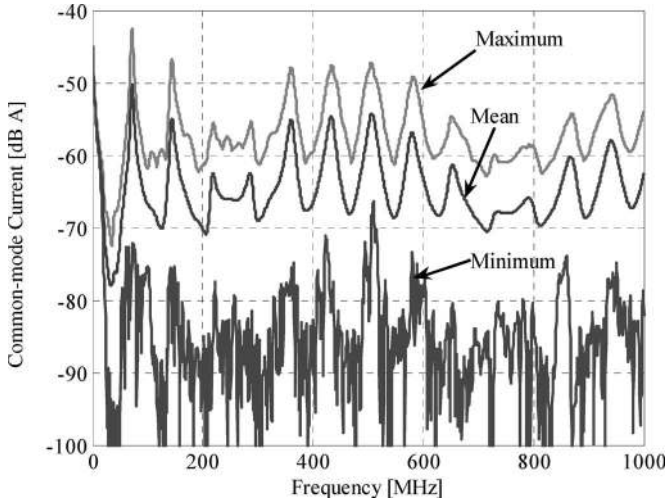

Fig. 5. Accumulated maximum, minimum, and average CM current from 128 simulations at point P1.

A. CM Current Prediction

Fig. 4 shows 128 simulated CM currents at point P1. The bold curves at the top and bottom in the figure are the accumulated maximum and minimum CM currents, respectively, among the 128 simulation results. Fig. 5 gives a better view of the statistical current distribution. According to the figures, the difference between the accumulated maximum and minimum CM current is 20 dB or greater for this bundle setup when the frequency is above 50 MHz. With an increasing frequency, the Q-factor of the CM currents decreases greatly because of skin effect loss and the dielectric loss of the PVC material.

Three randomly chosen CM currents among 128 simulations are plotted in Fig. 6. The patterns of the three CM currents reflect the random behavior of the cable bundles under test. In some frequency ranges, they have similar patterns, but in others, they are quite different. As shown in Fig. 7, the patterns of the simulated CM current at points P1, P2, and P3 with the same cable bundle are different because of the random nature of the bundle and the different terminations, even though points P1 and P3 are symmetric with respect to the midpoint of the bundle.

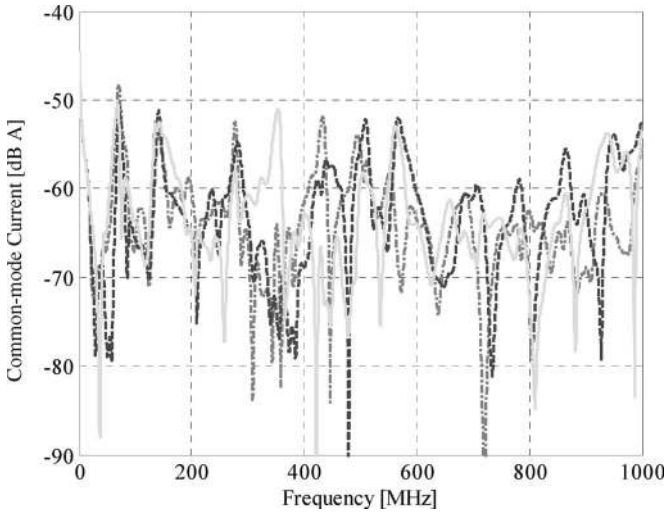

Fig. 6. Three simulated CM currents at point P1 with different bundle realizations.

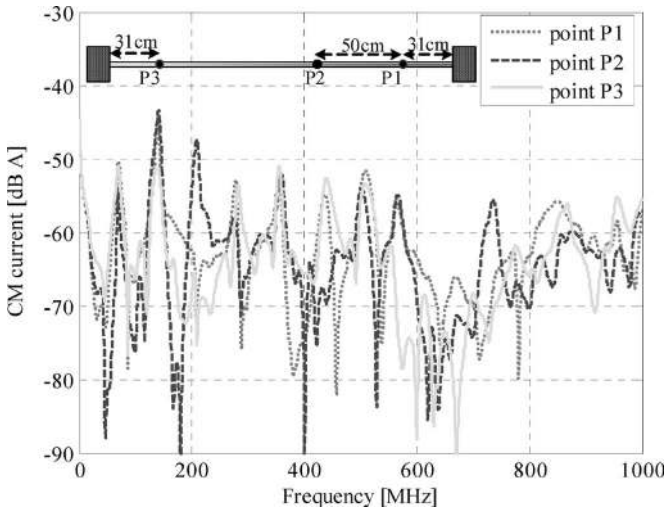

Fig. 7. Simulated CM current at point P1, P2, and P3 with the same cable bundle realizations.

B. Statistical Analysis

A statistical analysis was performed based on the simulation results. It is assumed that the statistical properties of the simulation results can be approximated with a Gaussian distribution. This assumption will be validated by comparing the histograms of the simulation data and the analytical probability density functions. With a Gaussian distribution, the mean and the standard deviation of the CM current at one cross section at a specific frequency can be evaluated as

$$\mu = \frac{1}{n}\sum_{i=1}^{n} x_i \tag{1}$$

$$\sigma^2 = \frac{1}{n-1}\sum_{i=1}^{n} (x_i - \mu)^2 \tag{2}$$

where n is the number of total simulations, and x_i is a specific simulation data at the specified frequency. The probability density function (PDF) can be evaluated as

$$f(x) = \frac{1}{\sqrt{2\pi}\sigma} e^{\frac{-[(x-\mu)^2]}{2\sigma^2}}. \tag{3}$$

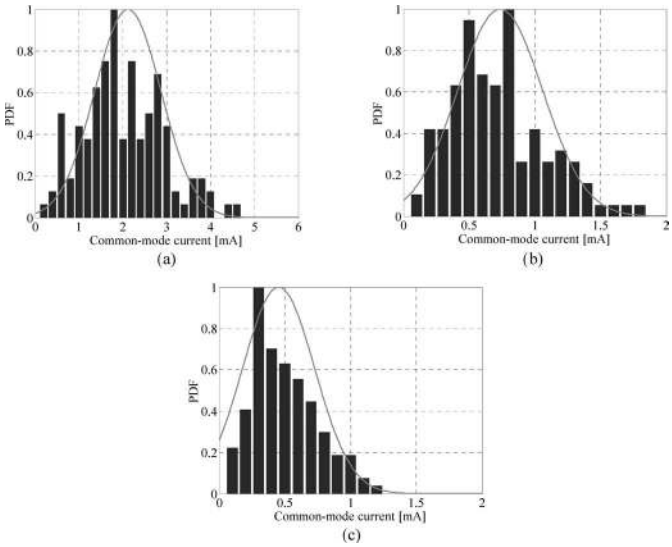

Fig. 8. Analytical probability density functions and the histograms at the corresponding frequencies: (a) 506 MHz, (b) 528 MHz, and (c) 550 MHz. The number of simulations is 128.

The normalized histograms and analytical PDFs evaluated with (3) at three frequencies are shown in Fig. 8 for the CM current at point P1. To be more representative of the general current distribution at all frequencies of interest, the first and third frequencies are intentionally chosen around a peak and a null of the CM current, and the second frequency is in between the peak and null frequencies. The generally good match between the histograms and the corresponding analytical PDFs indicates that a Gaussian distribution is suitable for statistically interpreting the simulation results. With finite simulations, the mean and standard deviation of the CM current can be extracted, and this information will be incorporated into a full-wave model to predict a range of E-/H-field with a given confidence level. For a Gaussian distribution, the probability of an event occurring within $\pm 3\sigma$ is 99.74%.

One critical issue for a statistical model is the minimum number of simulations or measurements that is sufficient to provide accurate statistical results. Better results can always be achieved with a larger number of simulations, but longer time and more computational resources are required. For instance, two HSPICE simulations running in parallel for this bundle setup took approximately 12 min with a computer that has a 3.2-GHz Pentium IV processor and 1-GB memory. The total simulation time for 16 simulations is approximately 1 h and 36 min, but it is approximately 13 h for 128 simulations. The difference in the simulation time is significant. To investigate a suitable number of simulations, a total of 128 simulations was performed. Fig. 9 shows the comparisons of the analytical PDFs and the corresponding histograms of the CM current at point P1 when the frequency is 506 MHz. With an increasing number of simulations, the histograms match the analytical PDF better, but it is still not clear

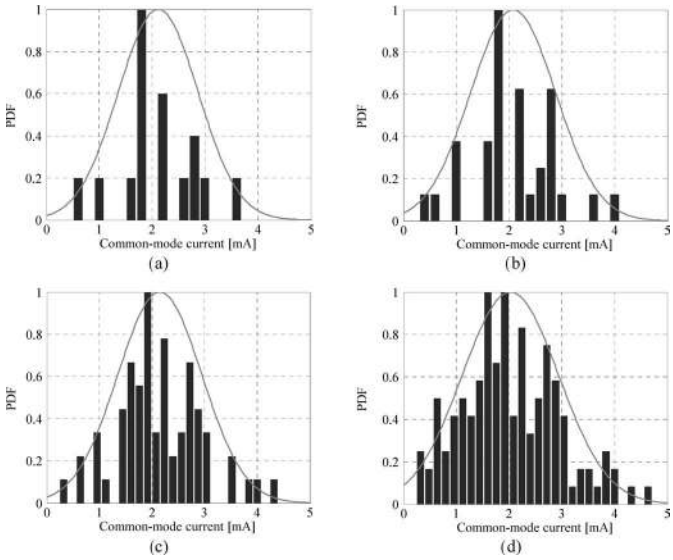

Fig. 9. Analytical PDFs and the histograms of the CM currents at 506 MHz when the number of the simulations are (a) 16, (b) 32, (c) 64, and (d) 128.

TABLE II
MEAN VALUES AND SIGMAS OF THE COMMON MODE CURRENTS WITH DIFFERENT NUMBER OF SIMULATIONS AT THE FREQUENCY OF 506 MHZ

Number of Simulations	16	32	64	128
Mean (mA)	2.11	2.07	2.15	2.03
Sigma (mA)	0.76	0.81	0.80	0.91

TABLE III
DIFFERENCE OF THE MEAN VALUES AND SIGMAS WITH RESPECT TO THAT OF 128 SIMULATIONS

Number of Simulations	16	32	64	128
Difference of mean (dB mA)	0.3	0.2	0.5	0 (ref.)
Difference of sigma (dB mA)	-1.6	-1.0	-1.1	0 (ref.)

what number of simulations is minimum, and yet sufficient. The mean values and standard deviations of the PDF are reported in Table II. The difference of the mean values and sigmas with respect to that of 128 simulations are reported in Table III. The small difference of the mean values and sigmas between 16 simulations and 128 simulations, which are 0.3 and –1.6 dB, respectively, shows that 16 is a suitable number for engineering purposes under this bundle setup, even though the mean and sigma calculation for such a small number of events is limiting. The number of simulations for general bundle setups may be different, and needs further investigation.

C. Electric Field Prediction

The CM current along the cable bundle is a primary contributor to the EMI. One efficient way to predict the system-level EMI resulting from a cable bundle on automotive platforms is to inject the CM current into a full-wave model as impressed current sources [8]. However, since the bundle is placed on a large metal plate for this setup, and there are no significant scatterers, the free-space Green's function, combined with image theory [9], is sufficient to predict the E- and H-fields. Herein, the current along every segment is approximated as a current filament with a constant magnitude and phase at the midpoint of the segment. Since the entire wire bundle is divided into 100 segments (each 2 cm long), which is less than one-tenth of the shortest wavelength of interest, CM current filaments along every segment are considered as infinitesimal current dipoles. The electric field obtained with the free-space Green's function approach at point P4 is shown in Fig. 10.

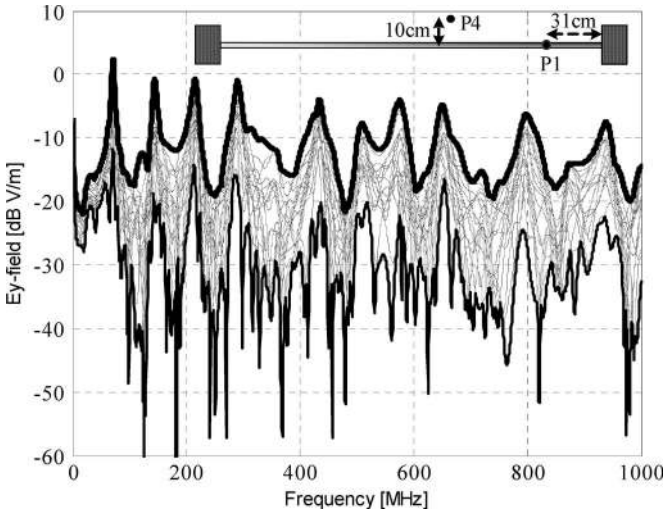

Fig. 10. Amplitude of 16 predicted E-fields at point P4.

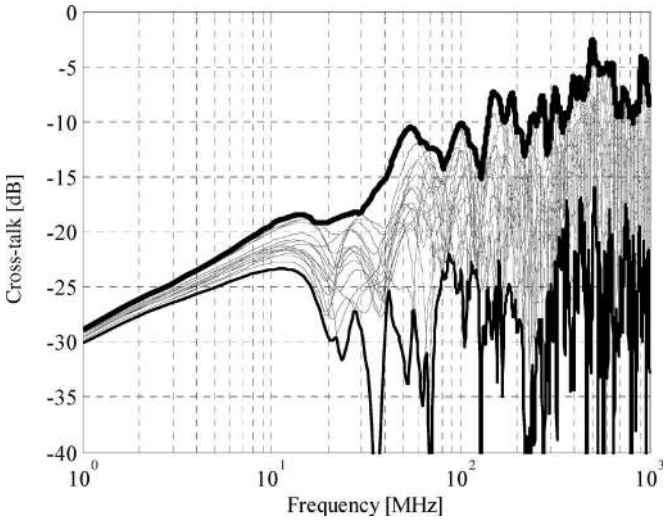

Fig. 11. Amplitude of the near-end crosstalk between wire 3 and wire 2 with 16 simulations.

D. Crosstalk Prediction

The voltage of each wire at two ends or any segments of the bundle can be easily simulated with a SPICE solver. The crosstalk between ith and jth wire can be evaluated with

$$H(f) = \frac{V_j(f)}{V_i(f)}. \tag{4}$$

Fig. 11 shows the near-end crosstalk between wire 3 and wire 2 with 16 simulations evaluated with (4). The thick curves at the top and bottom in the figure are the accumulated maximum and

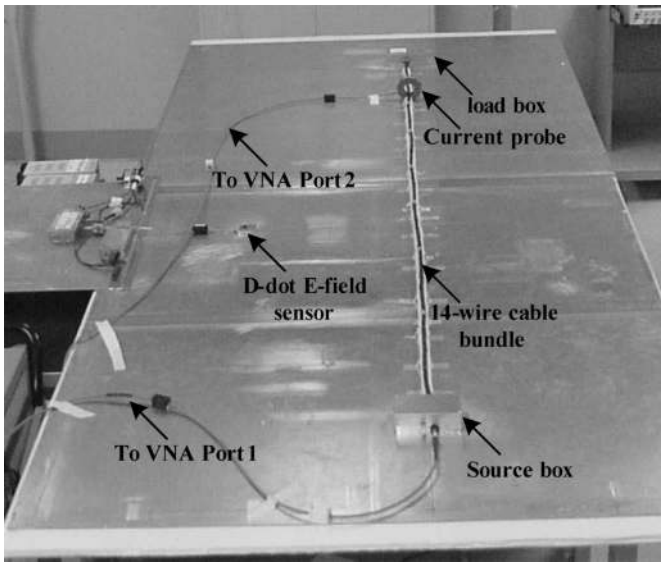

Fig. 12. Photograph of the measurement setup for a 14-wire, 2-m-long cable bundle over a large aluminum plate.

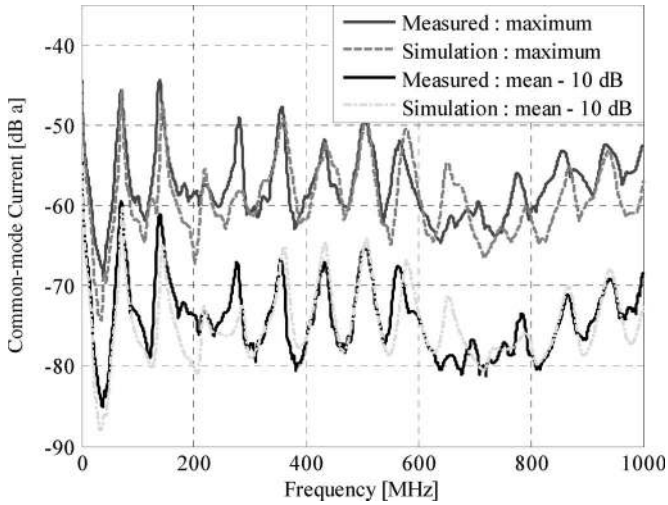

Fig. 13. Comparison of the measured and simulated maximum and average CM current at point P1. Note that both the simulated and measured average CM currents are shifted 10 dB lower from the original values for ease of comparison.

minimum results. Below 10 MHz, the slope of the envelop is approximately 10 dB/decade, which indicates that for electrical short lines, inductive coupling is still dominant because of the current-driven nature for feeding wire 2. For this bundle setup, there is only one wire whose source and load impedances are both relatively high.

The source and load impedances of all the other wires are either both low impedances or low–high-impedance combinations. The mutual coupling between wire 2 and all the wires effectively increases the impedance of wire 2, which reduces the feeding current along wire 2. This effect minimizes the inductive coupling between wire 2 and wire 3 from a theoretical value of 20 toward 10 dB/decade. Moreover, the mutual interactions between wire 3 and other wires except wire 2 also mitigate coupled current along wire 3 since all coupled current from wire 2 follows in the same direction; they tend to minimize each other due to the mutual coupling effect. When the frequency is beyond 20 MHz (electrically long), the amplitude of the crosstalk varies over a dynamic range greater than 20 dB, which means the crosstalk is very sensitive to the wire position disturbance.

IV. Experimental Validation

An experimental setup was constructed to validate the RDSI cable bundle model. A photograph of the measurement setup is shown in Fig. 12. The detailed geometry of the setup has been described in Section III. The bundle was connected to two aluminum boxes via two pairs of D-Subminiature Connectors. Wire 2 was connected to a subminiature type A (SMA) jack inside the source box, and all other wires were terminated with SMT resistors inside the source and load boxes. Port 1 of a vector network analyzer (HP 8753D) was used to feed wire 2 through the SMA jack, while port 2 of the vector network analyzer was connected to a current probe (Fisher F-61) or a laboratory-made electric field sensor for the CM current or the electric field measurements, respectively.

The effectiveness of the RDSI model is assessed by comparing the measured and simulated CM currents, the resulting electric fields, and the crosstalk. Since the RDSI algorithm is a statistical model, the 14-wire, 2-m-long cable bundle was randomly rewrapped 16 times, and all the measurements were reperformed 16 times accordingly. The measurement data and the simulation results are compared from a statistical point of view, which are in terms of accumulated maximum and mean values, and the standard deviations. Fig. 13 shows the comparison of the measured and simulated maximum and average CM currents among 16 results at point P1. The simulation results match the measurement results well, especially for the average CM current. The difference at most frequencies is less than 3 dB. This indicates that the RDSI cable bundle model can account for the random behavior of hand-assembled cable bundles from a statistical point of view. The small resonant frequency shifts at 280 and 560 MHz are due to the insertion impedance introduced by the current probe. The reasons for the missing resonances at 280 and 630 MHz might be the artifacts introduced by the current probe, the scattering from the termination boxes, laboratory objects, etc. These effects are not considered in the model. The remaining difference may be due to two factors. First, the finite number of the simulations and measurements may not be sufficient to achieve an optimum match; second, the measurement uncertainties may also contribute to some extent. Fig. 14 shows the comparison of the measured and simulated average $+ 3\sigma$ CM current at point P1. Herein, a Gaussian distribution was used to evaluate the standard deviations of the results at all frequencies. The good agreement of the standard deviations from the measurement results and the simulation data indicates that the Gaussian distribution is suitable for interpreting the RDSI simulation results. A piece of useful information from this figure is that within approximately 99.7% probability, the CM current at point P1 from an actual cable bundle is below the curve of the average $+ 3\sigma$ CM current. Fig. 15 shows the comparisons of the measured and predicted electric fields at point P4 obtained

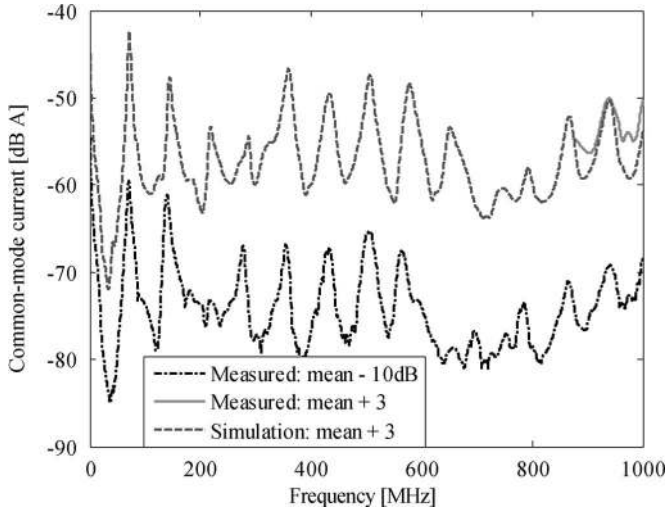

Fig. 14. Comparison of the measured and simulated average $+3\sigma$ CM current at point P1. Note that the measured average CM current is used as a reference and is shifted 10 dB lower from the original values for ease of comparison.

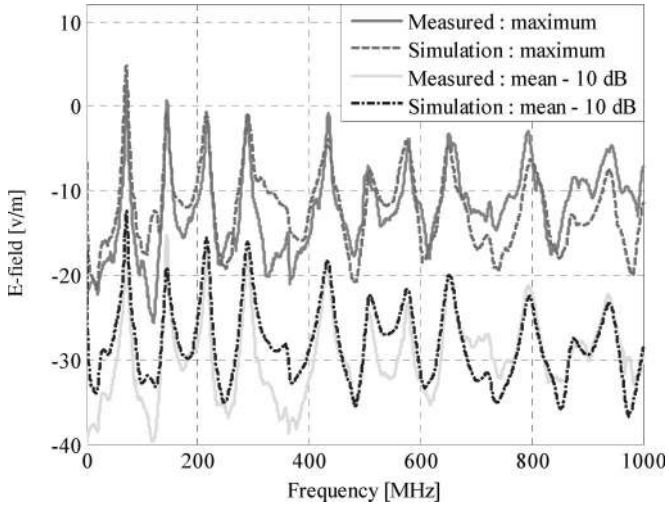

Fig. 15. Comparison of the measured and simulated maximum and average electric fields at point P4. Note that both the simulated and measured average E-field data are shifted 10 dB lower from the original values for ease of comparison.

with the free-space Green's function approach. The difference between the measured and simulated near E-fields is within 3 dB at most frequencies. This generally good match provides another way to validate the RDSI cable bundle model.

Crosstalk prediction is another important application of the proposed cable bundle model. Fig. 16 shows the comparisons of the measured and simulated maximum and average crosstalk between wire 2 and wire 3. An adequate match between the measurement and simulation results can be observed. The difference between the measurement and simulation results is less than 5 dB at most frequencies. The larger discrepancy between the simulation and measurement results for the crosstalk as compared to that of the CM current and the resulting E-field indicates that the crosstalk prediction is more sensitive to the wire position disturbance. The model parameters need to be further optimized to improve the crosstalk simulation.

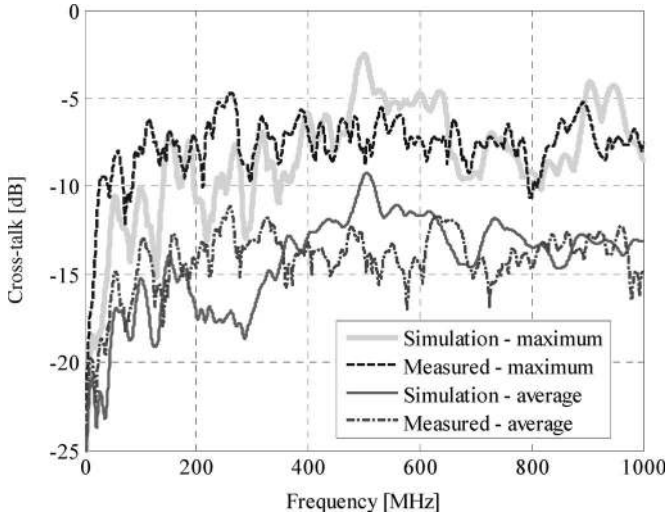

Fig. 16. Comparison of the measured and simulated maximum and average crosstalk between wire 2 and wire 3.

V. Engineering Implications

System performance can be predicted in many ways from an electromagnetic compatability (EMC) point of view, e.g., empirical equations, solving Maxwell's equations with boundary conditions, etc. However, for engineering purposes, the selected model should be simple, and yet sufficient to accurately represent the system of interest. The engineering considerations for modeling random cable bundles are investigated as follows.

A. Deterministic Versus Statistical Modeling

The necessity of employing the proposed statistical model instead of a deterministic model to simulate cable bundles is justified by comparing the CM currents simulated with the RDSI model and with a uniform bundle model (deterministic). For the RDSI model, the model parameters are as follows: the standard deviation of the wire position is 0.5; the length of spline segment is 20 cm; the subsegment length is 2 cm; and the skin effect, the dielectric loss, and the nonideal termination effects are considered. Sixteen simulations were performed. This case is referred to as the reference case. For deterministic modeling, the bundle is treated as a uniform, lossy bundle with ideal terminations. Fig. 17 compares the CM current at point P1 from the reference case and the uniform bundle case. The predicted CM current with the uniform bundle model approaches to the average CM current simulated with the RDSI statistical model. This means that there is a 50% chance that the CM current on an actual cable harness exceeds the predicted level, because for a Gaussian distribution, the probability of an event occurring within $-\infty$ to the mean is 50%. This deterministic simulation may lead to an optimistic engineering conclusion. Therefore, a statistical model is significant to account for the random behavior of hand-assembled cable bundles. This conclusion is also supported by the 20-dB or greater difference between the maximum and minimum CM current, as shown in Fig. 4.

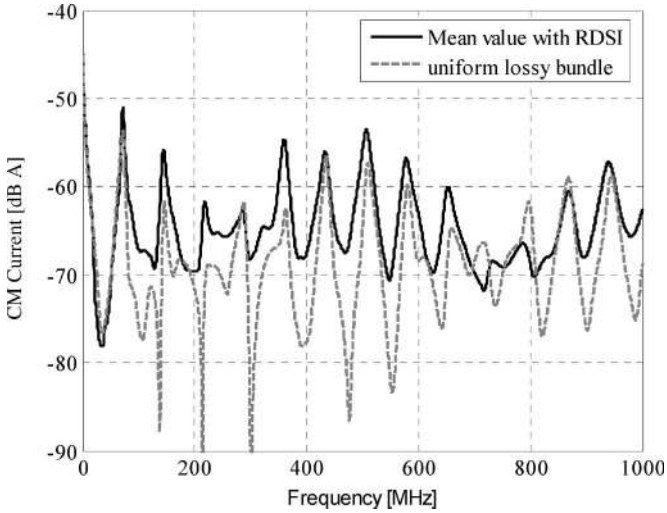

Fig. 17. Comparisons of the CM current at point P1 simulated with the RDSI algorithm and with a lossy, uniform bundle.

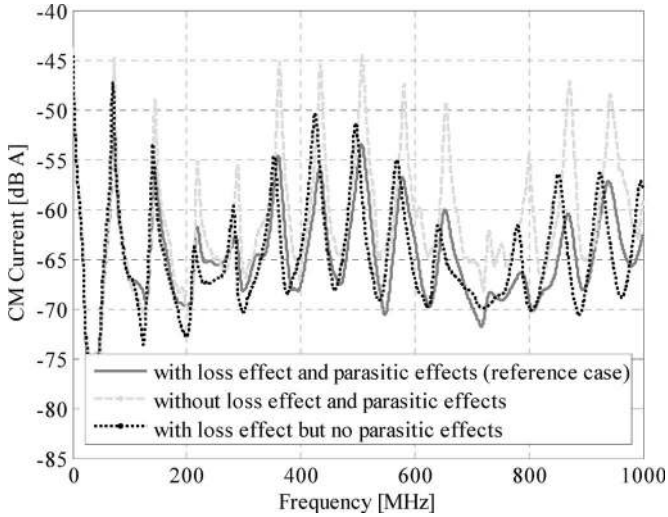

Fig. 18. Average CM current at point P1 for the reference case, and two cases with different configurations of parasitic effects and the loss effect.

B. Imapact of Loss Effects and Parasitic Effects

Two sets of simulations based on the RDSI algorithm were performed, and the results were compared to that of the reference case to investigate the impact of the loss effects and the parasitic effects, e.g., nonideal terminations and wrapping tape of the bundle, on the CM current. The number of simulations for each case is 16. For one set of simulations, the lossless bundles without wrapping tape and the nonideal termination effects were first considered. The dielectric loss of the PVC insulation material and the skin effect of the conductors were taken into account for the next set of simulations. For the reference case, all the parasitic effects and loss effects were considered. The model parameters of the two sets of simulations are the same as that of the reference case. Fig. 18 shows the comparisons of the average CM current at point P1, which clearly indicates the significant impact of the dielectric and skin effect losses on the CM current in terms of peak values and Q-factors of the resonances. The dielectric and skin effect losses are critical parameters that have to be considered for the cable harness modeling. They can mitigate the CM current of the order of 10 dB or more when the frequency is beyond a few tens of megahertz.

The nonideal terminations and the wrapping tape of the bundle have a nonnegligible impact on the CM current. Fig. 19 shows the modeling of the nonideal terminations with Ansoft 2-D field solver for p.u.l. L & C extraction. The comparison of the simulation results shows that when these parasitic effects were included in the model, the simulation results match the measurement results better in terms of peak values, resonant frequencies, and Q-factors of the CM current. These parasitic effects impact the CM current of the order of 4 dB for this bundle setup. These effects need to be considered in the model when accurate results are desired. For simulations without nonideal termination effects, the nonideal terminations at two ends of the bundle (3 cm long for each) were modeled with two 3-cm-long uniform bundles.

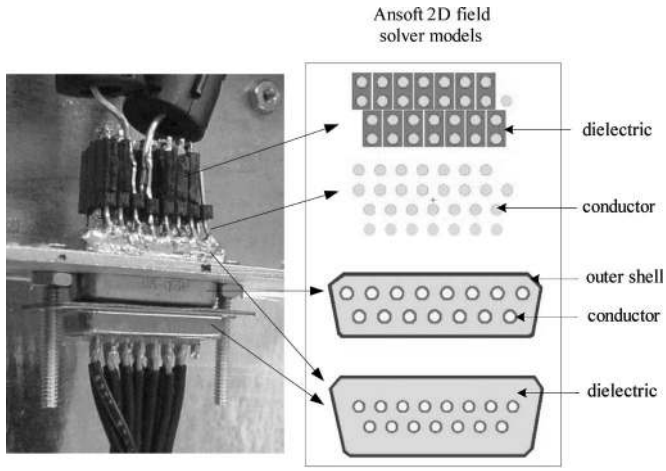

Fig. 19. Ansoft 2-D field solver models of each part of terminations for p.u.l. L & C extraction.

C. Influence of the RDSI Model Parameters

The standard deviation of the wire position and the length of the spline segments are two key parameters that control the amount of wire meandering through the bundle. Three cases with different standard deviations (sigma) of the wire positions, which are 0.1, 0.5, and 1.0, were performed and used to investigate the impact of the standard deviation of the wire position on the CM current along the bundle. The remaining parameters were same as that of the reference case. Sixteen simulations were performed for each case. As shown in Fig. 20, the comparisons of the measurement results and the average CM current with different sigmas show that with increasing standard deviations, the Q-factors of the CM current tend to decrease and approach that of the measurement results. The Q-factors of the CM current decrease greatly when the standard deviation increases from 0.1 to 0.5. However, there is no significant difference when the standard deviation increases from 0.5 to 1.0. The reason is illustrated in Fig. 21, which shows 3-D visualizations of wire

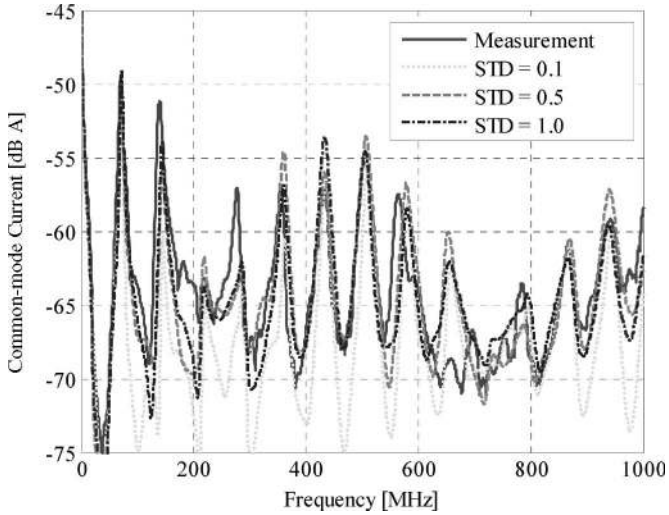

Fig. 20. Comparison of the average CM current at point P1 with different standard deviations of the wire position.

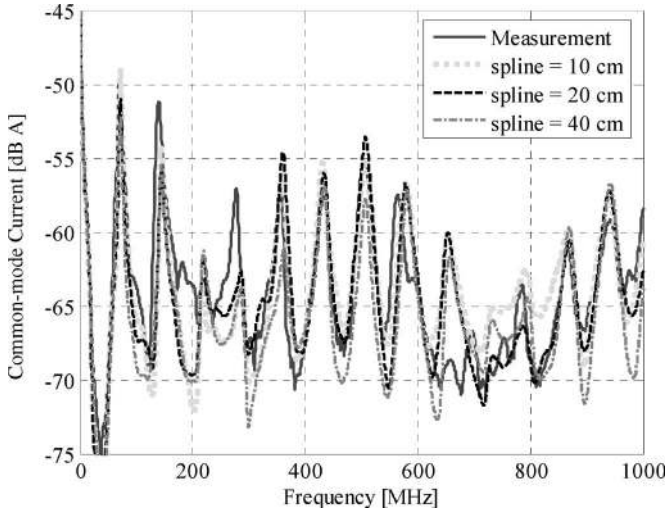

Fig. 22. Comparison of the average CM current with different spline segment lengths.

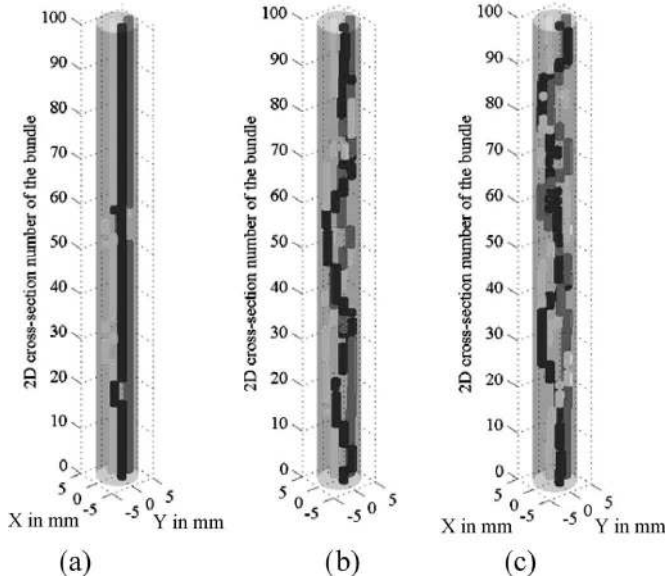

Fig. 21. Three-dimensional visualization of wire positions along the bundle with different standard deviations: (a) 0.1, (b) 0.5, and (c) 1.0. To preserve the readability, only three wires are plotted, which are wire 1, wire 6, and wire 11.

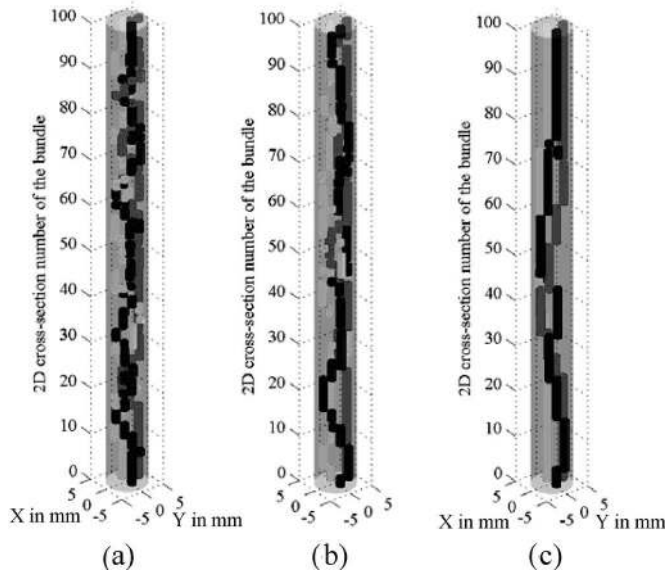

Fig. 23. Three-dimensional visualization of wire positions along the bundle with different spline segment lengths: (a) 10 cm, (b) 20 cm, and (c) 40 cm. To preserve the readability, only wire 1, wire 6, and wire 11 are plotted.

positions along the bundle with different standard deviations. As shown in the figure, the randomness of the wires nonlinearly increases with the standard deviation of the wire positions. The difference of the randomness of the wire bundle is not significant when the standard deviation increases from 0.5 to 1.0. For an actual cable bundle modeling, the standard deviation of the wire position should be adjusted according to the actual behavior of the cable harness.

The length of the spline segment is the other key parameter that controls the random behavior of the wire within the bundle. Three cases with different spline segment lengths, which are 10, 20, and 40 cm, respectively, are used to investigate the impact of the length of the spline segments on the CM current along the bundle. Each spline segment is divided into ten subsegments. The remaining parameters are same as that of the reference case. Fig. 22 shows that the spline segment length does not have a significant impact on the peak values of the CM current as long as the spline segment length is reasonable. For this case, when the spline segment length is 20 cm, the results are better in terms of peak values and Q-factors. Fig. 23 clearly shows the impact of the spline segment length on the randomness of the wires within the cable harness. The spline segment length influences the simulation results, but not significantly as long as it is reasonable. It is beneficial to choose the spline segment length according to the actual behavior of hand-assembled cable harnesses.

VI. Conclusion

The good agreement between the simulation results and the measurement data for the CM current along the cable bundle and the radiated electric field presented in the previous sections indicates that the proposed RDSI cable bundle model is suitable to account for the random behavior of hand-assembled cable bundles. With a finite number of simulations, the CM current along the bundle can be simulated with a SPICE-solver, and the average or maximum values of the CM currents and the variance can be obtained according to the simulation results. By injecting the average CM current and the standard deviation information into full-wave models [8], the electromagnetic fields can be efficiently computed within a desired confidence level. Herein, a Gaussian distribution is employed to approximate the statistical properties of the simulation results. The RDSI algorithm can also be used to predict the wire crosstalk within the bundles as well. Two model parameters, i.e., the standard deviation of the wire positions and the spline segment length, are the key parameters that control the randomness of the cable bundles. It is convenient to tune the randomness of the cable bundles by adjusting these two parameters according to the actual cable bundles.

The significance of a statistical model against a deterministic model for random bundle modeling is justified. The engineering decisions based on the results from deterministic simulations may be either too conservative or too optimistic. The investigations show that the dielectric and skin effect losses are two critical effects that have to be incorporated in the model. These effects have a significant impact on the CM current, and they can mitigate the CM current of the order of 10 dB. The parasitic effects, e.g., wrapping tape, nonideal terminations, etc., have nonnegligible impact on the simulation results. These effects may reduce the CM current of the order of several decibels.

References

[1] J. Nitsch and F. Gronwald, "Analytical solutions in nonuniform multiconductor transmission line theory," *IEEE Trans. Electromagn. Compat.*, vol. 41, no. 4, pp. 469–479, Nov. 1999.

[2] K. Lu, "An efficient method for analysis of arbitrary nonuniform transmission lines," *IEEE Trans. Microw. Theory Tech.*, vol. 45, no. 1, pp. 9–14, Jan. 1997.

[3] O. Gebele and H. D Bruns, "An efficient numerical method to solve the non-uniform MTL equation including field coupling," *IEEE Trans. Electromagn. Compat.*, vol. 2, pp. 648–652, Aug. 2003.

[4] S. Shiran, B. Reiser, and H. Cory, "A probabilistic model for the evaluation of coupling between transmission lines," *IEEE Trans. Electromagn. Compat.*, vol. 35, no. 3, pp. 387–393, Aug. 1993.

[5] S. Salio, F. Canavero, J. Lefebvre, and W. Tabbara, "Statistical description of signal propagation on random bundles of wires," presented at the 13th Int. Zurich Symp. Electromagn. Compat, Zurich, Switzerland, 1999.

[6] S. Salio, F. Canavero, D. Lecointe, and W. Tabbara, "Crosstalk prediction on wire bundles by Kriging approach," in *Proc. IEEE Int. Symp. Electromagn. Compat.*, Washington, DC, Aug. 2000, vol. 1, pp. 197–202.

[7] D. Weiner and G. Capraro, "A statistical approach to EMI theory and experiment, Part 2," presented at the 1987 Zurich Symp. Electromagn. Compat., Zurich, Switzerland, 1987.

[8] S. Sun, G. Liu, D. J. Pommerenke, J. L. Drewniak, R. W. Kautz, and C. Chen, "Anticipating EMI and on-board interference in automotive platforms," in *Proc. IEEE Int. Symp. Electromagn. Compat.*, vol. 3, Santa Clara, CA, Aug. 2004, vol. 3, pp. 792–797.

[9] C. Balanis, *Antenna Theory Analysis and Design*, 2nd ed. New York: Willey, 2002.

Shishuang Sun (S'03–M'07) received the B.S. and M.S. degrees in electrical engineering from Shanghai Jiao Tong University, Shanghai, China, in 1999 and 2002, respectively, and the Ph.D. degree in electrical engineering from the University of Missouri-Rolla, Rolla, in 2006.

He is currently a Senior Engineer with the Product Characterization Group, Altera Corporation, San Jose, CA. His current research interests include signal integrity in high-speed digital systems and power delivery network design and modeling.

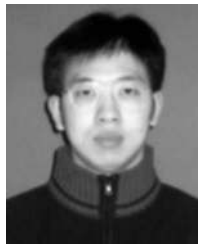

Geping Liu received the B.S. and M.S. degrees in electrical engineering from Tsinghua University, Beijing, China, in 1997 and 1999, respectively, and the Ph.D. degree in electrical engineering from the University of Missouri-Rolla, Rolla, in 2004.

From 2000 to 2004, he was a Graduate Research Assistant with the Electromagnetic Compatibility Laboratory, University of Missouri-Rolla. He is currently a Technical Staff Member with the Characterization Group, Altera Corporation, San Jose, CA. His current research interests include signal integrity, power integrity, and electromagnetic compatibility (EMC) designs in high-speed digital systems, and development and application of numerical and experimental methods in resolving signal integrity and EMC problems.

Dr. Liu received the Best DesignCon Paper Award from the International Electrotechnical Commission in 2006.

James L. Drewniak (S'85–M'90–SM'01) received the B.S., M.S., and Ph.D. degrees in electrical engineering from the University of Illinois, Urbana, in 1985, 1987, and 1991, respectively.

He joined the Electrical Engineering Department, University of Missouri-Rolla, Rolla, in 1991, where he is a Principal Faculty Member in the Electromagnetic Compatibility Laboratory. His current research and teaching interests include electromagnetic compatibility in high-speed digital and mixed-signal designs, electronic packaging, and electromagnetic compatibility in power-electronic-based systems.

Dr. Drewniak is the Chair of the Electromagnetic Compatibility Society Technical Committee TC-10 Signal Integrity.

David J. Pommerenke (M'98–SM'03) was born in Ann Arbor, MI, on April 11, 1962. He received the Diploma in electrical engineering and the Ph.D. degree in transient fields of electrostatic discharge (ESD) from the Technical University of Berlin, Berlin, Germany, in 1989 and 1995, respectively.

In 1989, he was with the Technical University of Berlin, where he was a Research and Teaching Assistant in electromagnetic compatibility (EMC) and high voltage. In 1996, he joined Hewlett Packard. In 2001, he became an Associate Professor with the Electromagnetic Compatibility Group, University of Missouri-Rolla, Rolla. His current research interest include EMC, ESD, numerical calculation, high-voltage partial discharge detection systems, electronics, and design of test and measurement equipment.

Dr. Pommerenke is a member of the International Electrotechnical Commission (IEC) TC77b WG-9, the working group that sets the IEC 61000-4-2 ESD test standard. He received the Distinguished Lecturer Award from the IEEE EMC Society for 2005–2006.